Journal of
Nanoscience and Nanotechnology
Vol. 13, 1011–1016, 2013

RESEARCH ARTICLE

Base Effects on Fluorescence and Surface-Enhanced Raman Scattering of Crystal Violet Adsorbed on Au Nanoparticles Surface

Penglan Chai, Jun Liu, Jun Tang*, Yunbo Shi, Chenyan Xue, and Huanfei Wen

National Key Laboratory for Electronic Measurement Technology, North University of China, Taiyuan, Shanxi Province, China

The Surface enhanced fluorescence (SEF) and Surface Enhanced Raman Scattering (SERS) of Au nanoparticle films deposited on Si and SiO_2 substrates are presented. From the experimental results, it is concluded that the fluorescence peak intensity changes in a similar way with the Raman intensity for the various substrates. Both the fluorescence and the Raman intensity were much stronger on SiO_2 substrate than on the Si substrate. That is due to the Crystal Violet (CV) adsorbed on the substrate having different refractive index effect the electrical field near the nanoparticles. The nanoparticle size effect on the Raman and fluorescence was also studied.

Keywords: SERS, SEF, Base Effects, Au Nanoparticles.

1. INTRODUCTION

Surface enhanced fluorescence (SEF) and Surface Enhanced Raman Scattering (SERS) are two promising techniques for detecting minimal quantities of biomolecules. Work in SERS reached a plateau approximately 10 years ago and became invigorated once again by the reports by Kneipp[1] and Nie[2] who reported that intense enough SERS emissions could be recorded under favourable circumstances to detect single molecules, that together with the quest for high-sensitivity molecular and especially biomolecular-sensing platforms, has returned SERS as a research field to the front burner so that there are arguably now more people working in SERS than ever before.

One of the most popular methods of SERS-substrates preparation in our days is deposition of Au or Ag nanoparticles on base. And the enhancement factors including particle size, shape, density were studied systematically.[3] At the same time, the base is the substrate of bio-chemical sensor. A lot of kind materials are used for base of SERS-substrate. In 2010, Panarina et al. reported *n*-type porous silicon as a new material for the fabrication of sensitive substrates for SERS.[4] Glass slides is one of the base material commonly used.[5] However, there are few reports about the effect of the base material on SERS and SEF.

In general, the observation of the SEF and SERS effect requires the localized surface plasmon modes. Ion sputtering is applied in this study to a set of Au thin films deposited simultaneously on different base materials (Si and SiO_2), in order to get insight into the effects of the base. For the Au thin films constant deposition conditions have been used, whereby only the deposition times have been varied, to get thin films of different thickness on different base material.

2. EXPERIMENTAL DETAILS

2.1. Nanoparticles Film Deposition

Au nanoparticles have been chosen for this study. The material used as a base was *P*-type silicon (with the refractive index of about 4.07) and 300 nm thick thermal SiO_2 (with the refractive index of about 1.54). Samples were cleaned ultrasonically with acetone and ethanol ten minute rinsed with deionized (DI) water, and dried in air.

For this study, Au films were deposited by DC sputtering on substrates of Silicon ((111)−0.51 mm thick) and SiO_2 (500(100) − 0.5 mm + 3000 Å thick), using a laboratory-size deposition system. The films were prepared with the substrate holder positioned at 70 mm from the target, using a DC current of 20 mA on the Gold target (99.99%). In this system, the base pressure is less than 20 mps and the chamber remains under ultra high vacuum even during sample transfer by means of a load-lock device. During deposition the working gas pressure was approximately constant (∼20 mps), and also to assure a

*Author to whom correspondence should be addressed.

practically constant deposition gas pressure of the vacuum chamber and current during film growth. The deposition time separately is 1 min, 2 min, 4 min and 6 min.

2.2. Chemical Preparation

Solution of biological macromolecules was prepared by adding 0.5 mg of CV to 10 mL of DI water. The samples were taken out after 2 hours immersion of the samples into a 10^{-5} mol/l solution of CV in DI water.

2.3. Instrumentation

The SERS spectra were recorded at a Renishaw Raman Microscope System invia, using the macro configuration equipped with a notch filter and an electrically refrigerated CCD camera. The Raman and Fluorescence emission spectra were recorded by the CCD camera. The 514.5 nm line of an Ar+ laser was used. The laser power at the sample was set to 5.0 mW. The exposure time is 50 s. Spectral resolution was 1 cm^{-1}, by selecting an appropriate slit (3000 l/mm). The maps reported here were recorded using a 50× microscope objective to focus the laser beam onto a spot of sample. The laser spot size was defocused and the Raman scattered light from a large surface area was collected. The auto force microscope (AFM) analysis was performed with a BY CSPM—3400 instrument in tapping mode, using PPP-NCHR NanoSensors silicon Al-coated caltilevers, with a resonant frequency of 300 KHz, and 40 Nm^{-1} elastic constant.

3. RESULTS AND DISCUSSION

3.1. Structural Properties

Two sets of samples were prepared by simultaneous deposition of the Au nanoparticle films on the different base (Si and SiO_2), by running four different deposition cycles varying the deposition time, to obtaine nanoparticles of different density and size.

In order to further study the reasons that the base effect, the relation between the nanoparticles and the base should be clarified. AFM images obtained from two sets of samples, give the opportunity to get an estimation of the size of each individual nanoparticle and eventually calculate the dimension distribution. Due to the lateral enlargement of the AFM measurements for the nanoparticles, the diameters of the nanoparticles calculated in this paper were mainly from the heights of the nanoparticles. Figure 1 shows the image obtained for deposition of 1 min, 2 min, 4 min and 6min on SiO_2 substrate. AFM measurements showed that the average size of the nanoparticles increase when the deposition time was increased.

Some indicative measures of Au nanoparticles height and density versus deposition time are given in Figure 2. It must be noticed that in the case of their samples, the average height of the nanoparticles deposited on SiO_2 substrate was increasing from 1.37 ± 0.17 nm to 5.26 ± 0.87 nm, and quit fast decreasing of the nanoparticles density from $1.52 \times 10^{11}/cm^2$ to $3.37 \times 10^{10}/cm^2$ the first, then the nanoparticles density is stable. For the deposition time is 6 min, the average height of the nanoparticles deposited on Si and SiO_2 substrate is 6.19 ± 1.95 nm and 5.26 ± 0.87 nm, and the nanoparticles density is $5.88 \times 10^{10}/cm^2$ and $6.22 \times 10^{10}/cm^2$ respectively. That is because the particles was dispersed on the surface of base at the beginning of deposition, then due to the larger particles are more energetically favored than smaller particles. The particles become larger generally, so the island is formed. As the increasing of deposition time, the islands connect with each other. The film formed at last. At the same time, the average height and the density of nanoparticles deposited on Si substrate were bigger than the nanoparticles deposited on SiO_2 substrate for deposition time shorter than 6 min. That is because the nanoparticles tend to possess one excess electron in the process of ion sputting. This excess electron allows the nanoparticles to be electrostatically manipulated. *P*-type Si provides the positive charges on the surface of the Si substrate and also provides the electrostatic interactions with negatively gold nanoparticles.

3.2. Raman and Fluorescence Analysis

The adsorbate was applied through incubation of the SERS substrates in 10^{-5} M solution of CV in DI water and dried for hours prior to the acquisition of the Raman or fluorescence spectra. SERS spectra of CV on Si and SiO_2 substrate with different deposition time and a typical dependence of Raman peak intensities versus deposition time are shown in Figure 3. CV adsorbed on the Au nanoparticles substrates prepared, exhibit the typical Raman signature superimposed on the fluorescence spectrum as shown in Figure 4. From the calculated intensity variations of the Raman and PL spectrum, it can be concluded that, as it is shown in Figures 3(c) and 4(c), a clear increasing of both Raman and PL intensity of CV on Si and SiO_2 substrate before deposition time was 4 min, and then the quit fast decreasing was observed. At the same time, both the fluorescence and the Raman intensity were much stronger on SiO_2 base when the deposition time was increased. For the Raman spectrum, such as the Raman peak of 1620 cm^{-1}, the intensity was increased from 649.05 ± 12.29 (a.u.) in the beginning to 5958.57 ± 94.08 (a.u.) after 2 min of deposition on SiO_2 base. Meanwhile for the PL intensity, the intensity was increased from 3377.99 ± 42.01 (a.u.) in the beginning to 44316.52 ± 450.19 (a.u.) after 2 min of deposition on SiO_2 base. At the beginning, for the smallest particles, localized surface-plasmon resonance (LSPR) extinction is dominated by absorption. So the intensity of raman is very

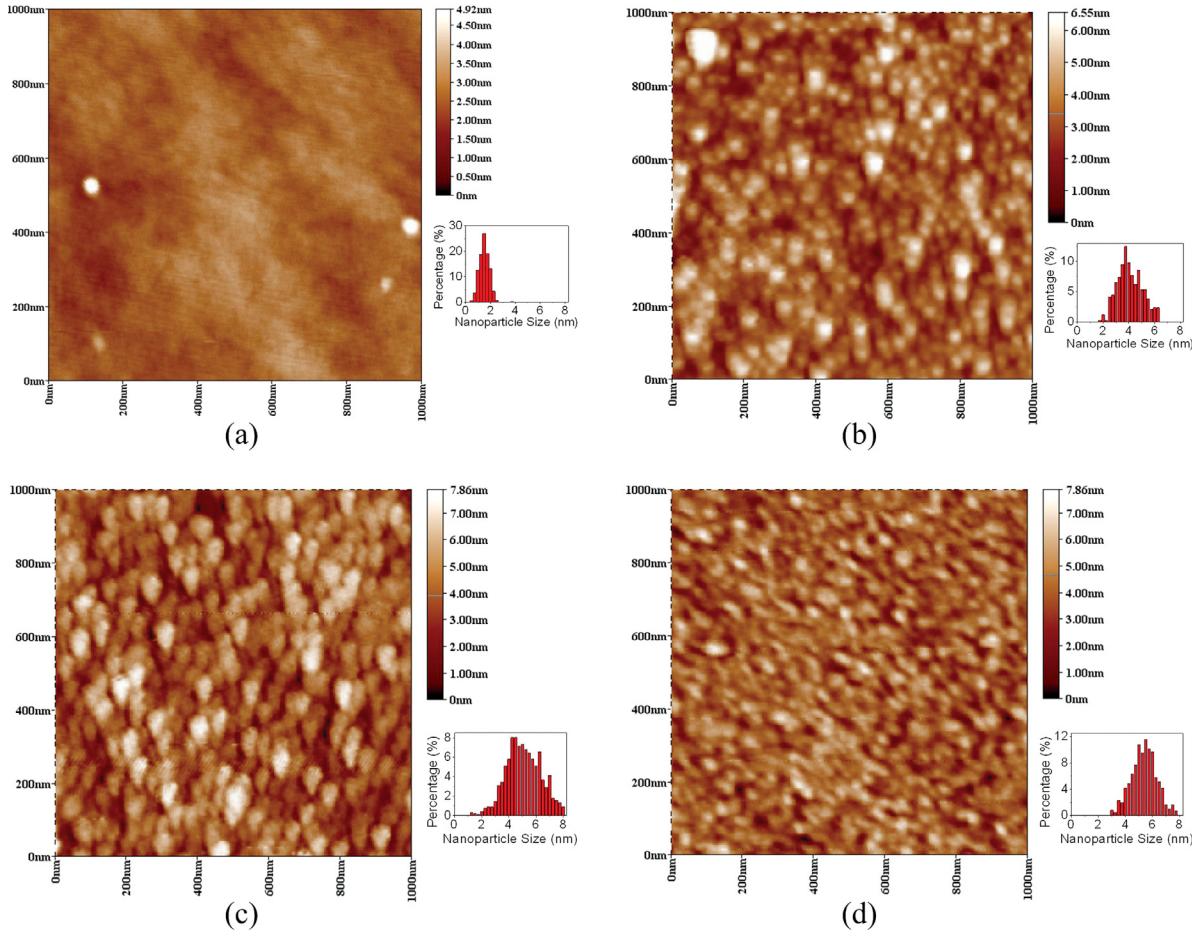

Fig. 1. AFM images of the nanoparticle films deposited on SiO_2 with different deposition time: (a) 1 min, (b) 2 min, (c) 4 min, (d) 6 min.

small at the deposition time is 1 min. And as particle size increases, scattering takes over.[6] At the same time, the AFM image of Figure 1 clearly shows that the nanoparticles film has a rather porous structure. Extremely intense local electromagnetic fields generated in the gaps between adjacent Au nanoparticles can strongly enhance the Raman scattering of probe molecules located in the gaps between the closely spaced Au nanoparticles.[7] Ashwin Gopinath et al. reported the Raman enhancement show a trend of increasing first and then the intensity of Raman decreasing when the nanoparticle size increasing.[3]

According to the publications,[8–9] electromagnetic field enhancement is also operative for the luminescence of molecules adsorbed on mental nanoparticles. According to

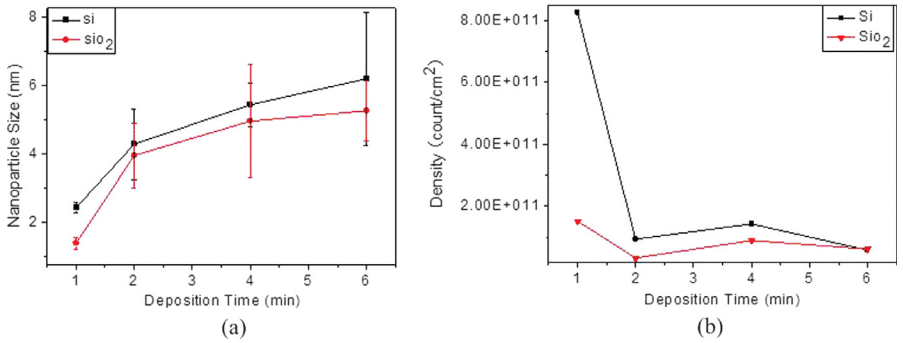

Fig. 2. The size and density of Au nanoparticles versus deposition time on two different substrate (Si and SiO_2): (a) Size; (b) Density.

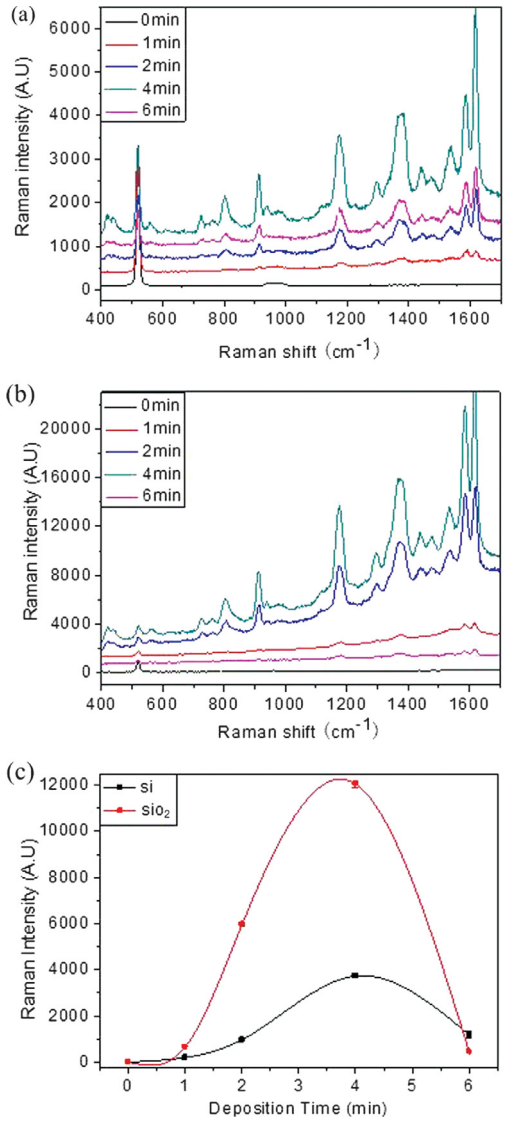

Fig. 3. SERS spectrum of the Basic Violet 3 on different substrates with different nanoparticle deposition time: (a) Raman spectrum of Au nanoparticles on Si substrates with different deposition time; (b) Raman spectrum of Au nanoparticles on SiO_2 substrates with different deposition time; (c) Raman intensity contrast on Si and SiO_2 substrate with different deposition time (1620 cm^{-1}).

a different but not opposite account, the fluorescence signal from the substrates prepared, depends on the balance between two competing phenomena: fluorescence quenching when molecules are adsorbed to Au nanoparticles and fluorescence enhancement, due to increased local fields experienced by molecules adsorbed to exposed base in the interparticle regions.[10] We surmise that in the case of first sample, where the density of the nanoparticles is small (see Fig. 1) the luminescence origin from CV adsorbed at the base, while for longer depositions the CV molecules are adsorbed at the Au nanoparticles.

According to the date shown in Figure 4(d), we observe the red-shift of the peak position at the beginning and then the blue-shift as the increasing of the deposition time. For the peak position of of CV on SiO_2 substrate, the peak position is increased from 636.02 nm in the beginning to 676.47 nm after 2 min of deposition on SiO_2 substrate, then the peak position is decreased from 676.99 nm to 655.92 nm. As the size increasing, the charge separation on the nanoparticles increases, leading to a lower frequency for the collective oscillation of electrons. The major dipole peak of the metal nanoparticles shows a continuous red-shift along with the increase in edge length of nanoparticles. In practice, the relationship between the LSPR peak position (in terms of wavelength) and the edge length of nanoparticles is more or less linear.[11] Once a specific peak position (and thus the edge length of nanoparticles) is reached, the synthesis can be quenched immediately.

4. DISCUSSION

According to the date shown in Figures 3 and 4, the fluorescence intensity followed the variation of Raman intensity for the various base prepared. The parallel evolution of Raman and fluorescence intensity with Au nanoparticles density indicated the existence of a common enhancement mechanism which becomes more prominent as the density of the Au nanoparticles increasing. CV adsorbed directly on SiO_2 base exhibits stronger fluorescence than Si base. When the molecules are in direct conduct with a flat gold surface, they interact through the near field with the free electrons of the metal and both the luminescence and the Raman spectra are quenched, at the same time the Raman and fluorescence intensity of CV on Si base is close to those on SiO_2 base, which is likely to reveals that the base effect had disappeared in SERS and SEF enhancement of deposition time is 6 min. Let us refer both to the SERS spectra of Figure 3(c) and to the SEF spectra reported in Figure 4(c). The raman intensity of deposition on SiO_2 correspond to an 6.17 fold of Si base. And the fluorescence of deposition on SiO_2 has a 5.8 fold of intensity of Si base. Through the comparative analysis of different adsorption base, we can know that the interaction between the base and the nanoparticles change the optical response.[12]

The SERS and SEF have common electromagnetic enhancement mechanism. The LSPR modes can contribute to larger SERS enhancement.[13–16] The description of aggregates of nanoparticles presents a number of additional complications compared with single particles, but in some cases, great simplifications are possible. Discrete dipole approximation (DDA) approach, with each particle in the aggregate represented by polarizable elements that are coupled together to determine the overall polarization response.[17] This approach has the advantage of allowing one to describe aggregates wherein the particles have arbitrary shapes, sizes, compositions, and geometrical

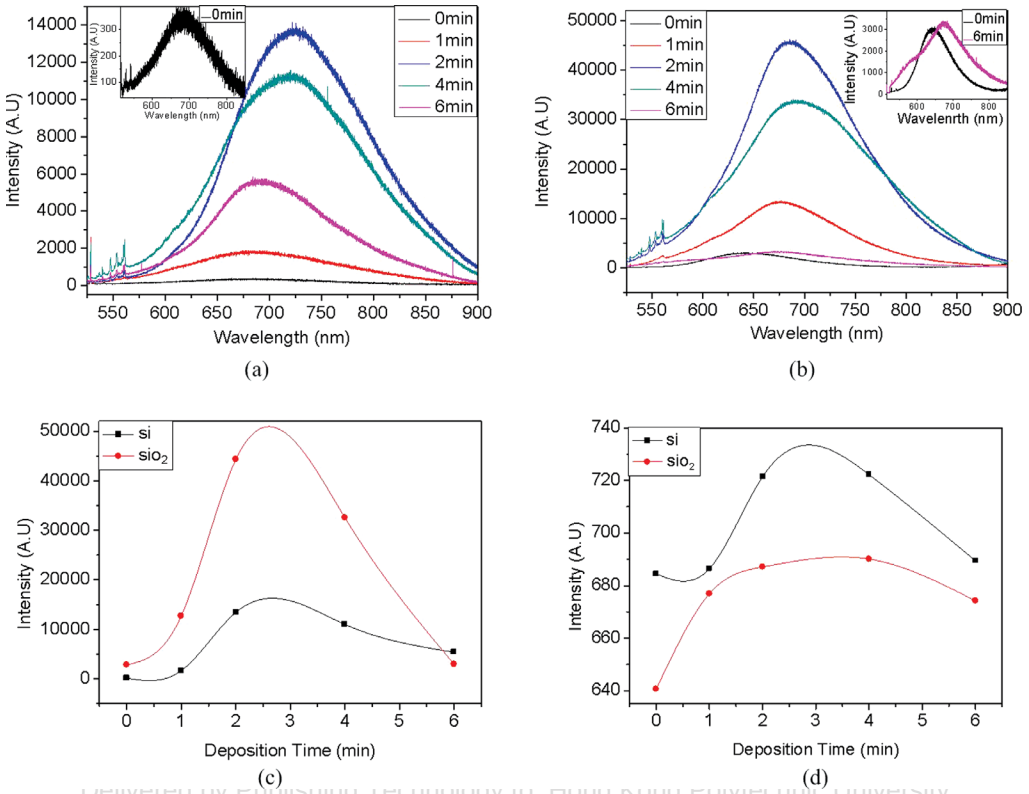

Fig. 4. SEF spectrum of the Basic Violet 3 on different substrates with different nanoparticle deposition time: (a) PL of Au nanoparticles on Si substrates with different deposition time; (b) PL of Au nanoparticles on SiO_2 substrates with different deposition time; (c) PL intensity contrast on Si and SiO_2 substrate with different deposition time; (d) PL peak position shift on Si and SiO_2 substrate with different deposition time.

arrangements. Effective refractive index (ERI) can easily be implemented in all DDA-based methods, including the ones proposed in Refs. [18–22]. At the same time, numerical results are reported by Simsek show that point-dipole method implemented with the proposed ERI approximation can provide a good estimate of the complete set of surface plasmon resonance modes in a multilayered medium.[23] According to Surface Plasmon Resonance Modes reported by Simsek, the base having different refractive index effect the relative intensity of SERS and SEF signals.

5. CONCLUSIONS

SERS and SEF were applied to study Base Effects on Fluorescence and Raman scattering of dye molecules adsorbed on Au mental surface. The purpose of work presented in this publication was to provide reference for develop bio-chemical sensor. In this paper, we examine some structural and optical properties of films of Au nanoparticles and examine the possibility of Raman and Fluorescence enhancement of different base. It was found that for CV, a clearly increase of both Raman and PL intensity was observed, which can be 6.17 fold of decreasing in Raman intensity and 5.8 fold of decreasing in PL intensity when the dye molecules are adsorbed at Au nanoparticles deposition on SiO_2 base. The similar dependence of the two intensities on the Au nanoparticle provides strong indication for a sole mechanism to account for both phenomena, which is related to LSPR modes. And ERI approximation can provide a good estimate of the complete set of surface plasmon resonance modes in different base.

Acknowledgments: This project is supported by the National Nature Science Foundation of China (91123016), National Nature Science Foundation of China (51105345).

References and Notes

1. K. Kneipp, H. Kneipp, I. Itzkan, R. R. Dasari, and M. S. Feld *J. Raman Spectrosc.* 29, 743 **(1998)**.
2. W. E. Doering and S. Nie, *J. Phys. Chem.* 106, 311 **(2001)**.
3. G. Ashwin, V. B. Svetlana, M. R. Björn, and D. N. Luca, *Opt. Express* 17, 3741 **(2009)**.
4. A. Y. Panarina, S. N. Terekhova, K. I. Kholostovb, and V. P. Bondarenkob, *Appl. Surf. Sci.* 256, 6969 **(2010)**.
5. Z. Yi, X. B. Xu, X. B. Li, J. S. Luo, W. D. Wu, Y. J. Tang, and Y. G. Yi, *App. Sur. Sci.* 256 5108 **(2011)**.
6. M. M. Kathryn and H. H. Jason, *Chem. Rev.* 111 3828 **(2011)**.

7. T. Qiu, X. L. Wu, J. C. Shen, P. C. T. Ha, and P. K. Chu, *Nanotechnology* 17, 5769 **(2006)**.
8. F. T. Lu, H. R. Zheng, and Y. Fang, *Progress in Chemistry* 19, 256 **(2007)**.
9. J. R. Lakowicz, *Anal. Biochem.* 298, 1 **(2001)**.
10. L. Gunnarsson, E. J. Bjerneld, H. Xu, S. Petronis, B. Kasemo, and M. Käll, *Appl. Phys. Lett.* 78, 802 **(2001)**.
11. S. E. Skrabalak, L. Au, X. D. Li, and Y. N. Xia, *Nature Protocols* 2, 2182 **(2007)**.
12. M. Á. Gracia-Pinilla, E. Pérez-Tijerina, J. A. Garcia, C. Fernández-Navarro, A. Tlahuice-Flores, S. Mejía-Rosales, J. M. Montejano-Carrizalez, and M. José-Yacamán, *J. Phys. Chem. C* 112, 13492 **(2008)**.
13. L. Lu, G. Sun, S. Xi, H. Wang, H. Zhang, T. Wang, and X. Zhou, *Langmuir* 19, 3074 **(2003)**.
14. A. M. Michaels, J. Jiang, and L. Brus, *J. Phys. Chem. B* 104, 11965 **(2000)**.
15. J. B. Jackson and N. J. Halas, *Proc. Natl. Acad. Sci.* 101, 17930 **(2004)**.
16. L. H. Lu, I. Randjelovic, R. Capek, N. Gaponik, J. H. Yang, H. J. Zhang, and A. Eychmüller, *Chem. Mater.* 17, 5731 **(2005)**.
17. G. C. Schatz, *J. Mol. Struc.-Theochem.* 573, 73 **(2001)**.
18. C. Noguez, *J. Phys. Chem. C* 111, 3806 **(2007)**.
19. S. A. Maier, M. L. Brongersma, P. G. Kik, and H. A. Atwater, *Phys. Rev. B* 65, 193408 **(2002)**.
20. W. H. Weber and G. W. Ford, *Phys. Rev. B* 70, 125429 **(2004)**.
21. A. F. Koenderink and A. Polman, *Phys. Rev. B* 74, 033402 **(2006)**.
22. A. F. Koenderink, R. D. Waele, J. C. Prangsma, and A. Polman, *Phys. Rev. B* 76, 201403 **(2007)**.
23. E. Simsek, *Plasmonics* 4, 223 **(2009)**.

Received: 12 September 2011. Accepted: 30 November 2011.

RESEARCH ARTICLE